THE JOURNAL OF BIOLOGICAL CHEMISTRY VOL. 285, NO. 16, pp. 12197–12209, April 16, 2010

Targeted Deletion of Hepatocyte ABCA1 Leads to Very Low Density Lipoprotein Triglyceride Overproduction and Low Density Lipoprotein Hypercatabolism*[S]

Received for publication, December 30, 2009, and in revised form, February 18, 2010 Published, JBC Papers in Press, February 23, 2010, DOI 10.1074/jbc.M109.096933

Soonkyu Chung[‡], Jenelle M. Timmins[‡], MyNgan Duong[‡], Chiara Degirolamo[‡], Shunxing Rong[‡], Janet K. Sawyer[‡], Roshni R. Singaraja[§], Michael R. Hayden[§], Nobuyo Maeda[¶], Lawrence L. Rudel[‡], Gregory S. Shelness[‡], and John S. Parks[‡1]

From the [‡]Department of Pathology/Section on Lipid Sciences, Wake Forest University Health Sciences, Winston-Salem, North Carolina 27157, the [§]Centre for Molecular Medicine and Therapeutics, University of British Columbia, Vancouver, British Columbia V5Z 4H4, Canada, and the [¶]Department of Pathology and Laboratory Medicine, University of North Carolina, Chapel Hill, North Carolina 27599

Loss of ABCA1 activity in Tangier disease (TD) is associated with abnormal apoB lipoprotein (Lp) metabolism in addition to the complete absence of high density lipoprotein (HDL). We used hepatocyte-specific ABCA1 knock-out (HSKO) mice to test the hypothesis that hepatic ABCA1 plays dual roles in regulating Lp metabolism and nascent HDL formation. HSKO mice recapitulated the TD lipid phenotype with postprandial hypertriglyceridemia, markedly decreased LDL, and near absence of HDL. Triglyceride (TG) secretion was 2-fold higher in HSKO compared with wild type mice, primarily due to secretion of larger TG-enriched VLDL secondary to reduced hepatic phosphatidylinositol 3-kinase signaling. HSKO mice also displayed delayed clearance of postprandial TG and reduced post-heparin plasma lipolytic activity. In addition, hepatic LDLr expression and plasma LDL catabolism were increased 2-fold in HSKO compared with wild type mice. Last, adenoviral repletion of hepatic ABCA1 in HSKO mice normalized plasma VLDL TG and hepatic phosphatidylinositol 3-kinase signaling, with a partial recovery of HDL cholesterol levels, providing evidence that hepatic ABCA1 is involved in the reciprocal regulation of apoB Lp production and HDL formation. These findings suggest that altered apoB Lp metabolism in TD subjects may result from hepatic VLDL TG overproduction and increased hepatic LDLr expression and highlight hepatic ABCA1 as an important regulatory factor for apoB-containing Lp metabolism.

ABCA1 (ATP-binding cassette transporter A1) is indispensable in the initial steps of high density lipoprotein (HDL)[2] formation and the process of reverse cholesterol transport from peripheral tissues to the liver. ABCA1 is expressed in many cells; however, hepatocytes make the single most important contribution to plasma HDL concentration (1–3). Mutations in *ABCA1* in humans cause Tangier disease (TD), an autosomal recessive disorder characterized by severe HDL deficiency, rapid plasma clearance of HDL and apoA-I, sterol deposition in tissues, and premature coronary atherosclerosis (4–7).

In addition to HDL deficiency, TD subjects have significantly elevated plasma TG and a 50% reduction in LDL cholesterol concentrations (4, 8). The TG phenotype in TD disease is complicated, with most, but not all, TD subjects displaying elevated fasting or postprandial TG elevations (9). Clee *et al.* (8) reported an inverse relationship between dysfunctional ABCA1 alleles and plasma TG concentrations. In addition, data from case reports of 59 Tangier patients show variable TG concentrations, with mean, median, minimum, and maximum concentrations of 210, 175, 40, and 580 mg/dl, respectively (4). The underlying mechanisms for the increased plasma TG and decreased LDL concentrations in TD subjects have not been established. In one study, apoA-II enrichment of VLDL of TD subjects was proposed to result in reduced reactivity of VLDL with lipoprotein lipase (LPL) (9, 10). Another study suggested that ABCA1-dependent cholesterol efflux decreases VLDL secretion from murine hepatocytes by limiting cholesterol availability for VLDL assembly (11). However, whether deficiency of ABCA1 is associated with increased apoB lipoprotein secretion *in vivo* is unknown.

Recently, we reported that silencing of ABCA1 in rat hepatoma cells is associated with PI3K-dependent enhanced secretion of TG-enriched VLDL (12), suggesting a potential role of hepatic ABCA1 expression in VLDL assembly and secretion. To determine whether hepatic ABCA1 expression affects VLDL secretion *in vivo*, we used loss of function and gain of function strategies with hepatocyte-specific gene targeting of

* This work was supported, in whole or in part, by National Institutes of Health Grants P01 HL 49373 (to L. L. R., G. S. S., and J. S. P.), R01 HL 54176 (to J. S. P.), P50 AT 27820 (to J. S. P.), and R01 HL 94525 (to J. S. P.). This work was also supported by American Heart Association Mid-Atlantic Affiliate Postdoctoral Fellowship 0825445E (to S. C.).

[S] The on-line version of this article (available at http://www.jbc.org) contains supplemental Table 1 and Fig. 1.

[1] To whom correspondence should be addressed: Dept. of Pathology/Section on Lipid Sciences, Wake Forest University Health Sciences, Medical Center Blvd., Winston-Salem, NC 27157-1040. Tel.: 336-716-2145; Fax: 336-716-6279; E-mail: jparks@wfubmc.edu.

[2] The abbreviations used are: HDL, high density lipoprotein; LDL, low density lipoprotein; apo, apolipoprotein; FCR, fractional catabolic rate; MTP, microsomal triglyceride transfer protein; PI3K, phosphatidylinositol 3-kinase; TG, triglyceride; VLDL, very low density lipoprotein; LPL, lipoprotein lipase; TD, Tangier disease; FPLC, fast protein liquid chromatography; LDLr, LDL receptor; LDLrKO, LDLr knock-out; Ad-ABCA1 and -AP, adenoviruses expressing full-length human ABCA1 and alkaline phosphatase, respectively; WT, wild type; HSKO, hepatocyte-specific ABCA1 knock-out; GAPDH, glyceraldehyde-3-phosphate dehydrogenase; HL, hepatic lipase; TPC, total plasma cholesterol; Lp, lipoprotein; TC, total cholesterol.

ABCA1 and adenoviral overexpression of human ABCA1, respectively. We demonstrate that targeted inactivation of hepatic ABCA1 increases VLDL production and LDL clearance, recapitulating the TD lipid phenotype, and that adenoviral rescue of ABCA1 reverses the elevated plasma TG phenotype. These studies highlight a novel and important role for hepatic ABCA1 in regulating apoB Lp metabolism.

EXPERIMENTAL PROCEDURES

Animals and Diet—Generation and genotyping of HSKO (albumin Cre^+, $ABCA1^{flox/flox}$), hetero-HSKO (albumin Cre^+, $ABCA1^{flox/+}$), and wild type control (albumin Cre^+, $ABCA1^{+/+}$) mice were performed as described previously (1). The HSKO mice used for this study were backcrossed into the C57BL/6 background and determined to be >99% in that background by genome-wide screens using 134 single nucleotide polymorphisms that were polymorphic between the C57BL/6 and 129/SvEv strains and spaced ~20 megabase pairs across the mouse genome. HSKO mice were also crossed with LDL receptor knock-out (LDLrKO) mice (Jackson Laboratories). The mice were housed in the Wake Forest University Health Sciences animal facility with a 12-h light (6 a.m. to 6 p.m.)/12-h dark cycle and maintained on a chow diet (Prolab RMH3000 rodent diet, LabDiet). In most studies, 12–16-week-old male mice were used. In one study, 8-week-old mice were fed an HF diet containing 45% calories from fat (90% from lard), 35% calories from carbohydrate (50% from sucrose), and 20% from protein for 8 weeks. All protocols and procedures were approved by the Wake Forest University Health Sciences Animal Care and Use Committee.

Analysis of Plasma and Liver Lipids—Plasma was collected by tail bleeding of 6-h fasted or non-fasted mice. To determine lipoprotein lipid distribution, pooled plasmas were either fractionated by two Superose 6 FPLC columns (1 × 30 cm) in series (flow rate 0.5 ml/min; Fig. 1*D*) (1) or by a high resolution Superose 6™ FPLC column (10/300GL, Amersham Biosciences; flow rate 0.5 ml/min; see Fig. 6, *D–F*). Fractions eluting from the columns were used for enzymatic determination of total plasma cholesterol (TPC) and TG. In Fig. 5*F*, TPC distribution in whole plasma was determined using a high resolution Superose 6 column (1 × 30 cm) and an online cholesterol analyzer (Elite La Chrome, Hitachi). Total cholesterol and triglyceride concentrations were determined by an enzymatic colorimetric assay using a commercial kit (Chol and Trig/GB, Roche Applied Science). For the free fatty acid composition analysis, lipid extracts from liver were fractionated into cholesteryl ester, TG, and phospholipid bands by TLC, and then each fraction was methylated and analyzed by gas-liquid chromatography (13). For the quantification of hepatic free fatty acid content, liver lipid extracts (Bligh-Dyer extraction) were dried down under N_2, solubilized with 1% Triton X-100 (14), and then quantified using a commercial NEFA assay kit (Wako).

Liver Perfusion—Recirculating liver perfusion was carried out as described previously (15). Ten ml of perfusate medium with erythrocytes (10% hematocrit) were pumped through livers at 1 ml/min for 3 h. Every 30 min during perfusion, 1 ml of perfusate was collected, and perfusate volume was replenished with fresh perfusate. The collected perfusate was centrifuged (1,100 × *g* for 30 min) to pellet erythrocytes and perfusate plasma was then assayed for TG concentration using an enzymatic assay as described previously (15). A plot was then made of perfusion time *versus* TG concentration for each animal; lipid accumulation rates were obtained from the slope of the line of best fit, determined by linear regression analysis using GraphPad Prism 5® software (GraphPad Software, Inc., San Diego, CA).

VLDL Subfractionation and Particle Size Analysis—For plasma lipoprotein fractionation, 200 μl of pooled plasma (n = 3 per genotype) was first adjusted to d = 1.10 g/ml with solid KBr in 4 ml of saline. Plasma was overlaid with 3 ml of d = 1.065 g/ml NaBr, 3 ml of d = 1.02 g/ml NaBr, and 3 ml of d = 1.006 g/ml NaCl in a Beckman SW40 centrifuge tube. After ultracentrifugation at 40,000 rpm for 148 min at 20 °C, VLDL1 (S_f > 100) was collected from the top 1 ml of the gradient. Following a subsequent ultracentrifugation at 37,000 rpm for 18 h at 15 °C, $VLDL_2$ (S_f20–100) and other lipoproteins were collected from the top into 11 fractions (1 ml each). TG concentration in each fraction was determined by enzymatic assay. VLDL size from an equal volume of pooled VLDL1 and VLDL2 was analyzed using a Zetasizer Nano S® dynamic light scattering instrument (Malvern). Particle sizes are reported as median peak diameter using volume analysis.

In Vivo Determination of VLDL TG and ApoB Secretion Rate—After a 4-h fast, male mice (n = 3 of each genotype) were anesthetized and injected in the peritoneal cavity with poloxamer 407 (1,000 mg/kg; Sigma), to block lipolysis and with [^{3}H]oleate (5 μCi/g body weight) and [^{35}S]Cys/Met (7 μCi/g body weight) as tracers of TG and protein synthesis, respectively (16, 17). To study the effect of *in vivo* inhibition of PI3K on VLDL TG and apoB production, mice were injected with the PI3K inhibitor wortmannin (1.5 μg/g body weight) 1 h prior to detergent injection as described previously (18). Fifty μl of blood were collected from anesthetized mice by retro-orbital bleeding at 0, 1, 2, and 4 h after injection. Plasma was harvested from the blood samples and used to quantify TG mass by enzymatic assay and radiolabel incorporation into newly secreted VLDL TG and apoB. Briefly, plasma was lipid-extracted, TG was fractionated by thin layer chromatography, and radiolabel in the TG band was quantified by liquid scintillation counting. TG secretion rates were derived from the slope of the line of best fit of time *versus* plasma [^{3}H]TG plots for each individual animal using GraphPad Prism 5. To measure secretion of newly synthesized apoB, 10 μl of the terminal plasma sample were immunoprecipitated with goat anti-human apoB antiserum (5 μg) in buffer containing 1% Triton X-100, 0.1% SDS, 0.5% sodium deoxycholate, 0.2% bovine serum albumin, protease inhibitors, and phosphatase inhibitor (*i.e.* immunoprecipitation buffer). After 18 h of incubation of the samples with rotation at 4 °C, 20 μl of protein G beads (50:50 slurry; Amersham Biosciences) were added for 2 h. Beads were collected by centrifugation at 10,000 rpm for 10 s and washed three times with lysis buffer. Proteins were eluted from the beads by heating (70 °C for 10 min) in SDS-PAGE sample buffer and fractionated by 4–8% gradient SDS-PAGE. Gels were then dried and visualized with a PhosphorImager.

Plasma Lipase Activity—To prepare post-heparin plasma, mice were first anesthetized, and then 300 units/kg heparin was injected via the tail vein ($n = 7–8$ per genotype). Blood was collected by cardiac puncture 15 min after heparin injection using a heparin-coated syringe. Hepatic lipase (HL) and LPL activities were measured in the post-heparin plasma (20 μl) using a radiolabeled triolein-Triton X-100 mixed micellar substrate as described previously (19). HL activity was measured as the activity in the presence of 1 M NaCl or in the absence of apoC-II activator. LPL activity was calculated as total activity minus HL activity. Lipolytic activities were expressed as μmol of fatty acid released/h/ml of plasma.

Postprandial Lipemia Study—Age- and body weight-matched male mice ($n = 4$ of each genotype) were fasted for 4 h, beginning at 6:00 a.m. For basal level TG measurement, 20 μl of blood was collected from the tail vein, prior to oral administration of 150 μl of olive oil. Subsequent bleeds followed at 0.5, 1, 2, 4, and 8 h post-gavage. Plasma concentrations of triglycerides were determined by an enzymatic assay as described above.

Hepatic PI3K Activation—To determine the activation of hepatic PI3K after acute insulin injection, mice were anesthetized with ketamine/xylazine, the portal vein was exposed, and 5 units insulin/kg body weight were injected. Five min later, liver was isolated and snap-frozen in liquid N_2 and kept at −80 °C until analyses were performed. Liver homogenates were prepared in the presence of protease/phosphatase inhibitor mixture (Sigma) and subsequently used for Western blot analysis of total PI3K p85 and phospho-PI3K 85 expression. For the fast/refeeding studies, mice were moved to individual clean cages (with free access to water) and fasted for 15 h, re-fed for 2 h, and then fasted for an additional 2 h to allow clearance of chylomicrons (*i.e.* refed group) before the mice were euthanized for liver collection. The fasted group was fasted for a total of 19 h before liver collection.

Primary hepatocytes from WT and HSKO mice were isolated as described previously (1) and used for PI3K activation and TG secretion studies. Briefly, the portal vein was cannulated, and the liver was perfused at a rate of 4 ml/min with a calcium- and magnesium-free buffer (10 mM HEPES, pH 7.4, 0.5 mM EDTA), followed by a collagenase solution (0.3 mg/ml collagenase I, Worthington). Hepatocytes released from the liver capsule and intact hepatocytes were isolated by two rounds of centrifugation at 50 × *g* for 5 min. Cells were plated into 35-mm dishes precoated with collagen (Sigma) at a density of 0.5×10^6 cells/dish in William's E medium containing 5% fetal bovine serum, 2 mM L-glutamine, 0.1 nM insulin (Sigma), 100 units/ml penicillin, and 100 μg/ml streptomycin. The PI3K activation was evaluated as mentioned above, and TG secretion were measured as we described previously (12).

LDL Turnover—LDL was isolated from 2 ml of LDLrKO plasma by sequential ultracentrifugation (Beckman Instruments, Palo Alto, CA) at $d = 1.019–1.063$ g/ml. The isolated mouse LDL preparation was radiolabeled with ^{125}I using the iodine monochloride method (20). Specific activity of the ^{125}I-LDL tracer was 308 cpm/ng protein, trichloroacetic acid-precipitable ^{125}I radioactivity was 97%, and lipid radiolabeling was negligible. The ^{125}I-LDL tracer also eluted with authentic LDL on a Superose 6 FPLC column. Recipient mice ($n = 4$/genotype) were anesthetized with isoflurane, and 0.5×10^6 cpm of the radiolabeled tracer were injected via the tail vein. Blood samples (30 μl) were drawn at 2, 10, and 30 min and 1, 3, 6, and 22 h after tracer injection by retro-orbital bleeding of anesthetized mice. ^{125}I-apoB (apoB-48 plus apoB-100) was precipitated from 15 μl of plasma using isopropyl alcohol, with human LDL (100 μg) as a carrier (17), and ^{125}I radiolabel was determined by γ-scintillation spectrometry. Turnover curves were plotted as a percentage of the 2-min plasma radioactivity remaining in plasma after injection of the tracers. Fractional catabolic rate (FCR) was calculated for individual plasma die-away curves using a biexponential curve-fitting program in GraphPad Prism 5.

Adenoviral Overexpression of hABCA1—Adenoviruses expressing full-length human ABCA1 (Ad-ABCA1) and alkaline phosphatase (Ad-AP) were generated was previously described (21, 22). The titration of recombinant adenovirus was performed using a commercial titration kit (Adeno-X™ Rapid Titer kit, Clonetech). Preinfection blood samples of non-fasted WT and HSKO mice fed a HF diet for 8 weeks were collected at 9:00 a.m. via tail vein bleeding. Adenoviral vectors were diluted in sterile PBS and intravenously delivered to WT and HSKO mice ($n = 4$/group) at a dose of 3×10^8 infectious units/mouse (21, 22). Three days after Ad-AP or Ad-ABCA1 infection, blood and liver samples were collected at 9:00 a.m. from the non-fasted WT and HSKO recipient mice.

Real-time PCR Analysis—Total RNA was isolated from liver of age-matched male mice using TRIzol (Invitrogen), and real-time PCR was performed as described previously (23). Primer sequences for ABCA1, ABCG1, SRBI, SREBP2, LXRα, LXRβ, and GAPDH expression were the same as reported previously (23). Sequences for ABCG5, LRP, LDLr, SREBP1c, PPARα, PPARγ, PGC1α, and FXRα are summarized in supplemental Table 1. GAPDH was used as an endogenous control.

Western Blotting—Mouse liver extract was prepared by homogenizing ~500 mg of frozen liver with a Polytron homogenizer in radioimmune precipitation lysis buffer containing protease inhibitor and phosphatase inhibitor mixture (Sigma). Western blots were performed as previously described (1). Polyclonal antibodies targeting phospho-PI3K p55/p85, phospho-Akt (Ser^{473}), and total Akt were purchased from Cell Signaling Technology. Antibodies against human apoB and mouse apoA-I were purchased from Biodesign. Antibody against endothelial lipase was purchased from Cayman Chemical. Polyclonal antibodies directed at LDLr and apoE were provided by Dr. Liqing Yu (Wake Forest University Health Sciences).

Statistics—Results are presented as means ± S.E. Data were statistically analyzed using Student's *t* test or one-way analysis of variance with Tukey's multiple comparisons.

RESULTS

Targeted Deletion of Hepatocyte ABCA1 Results in Postprandial Hypertriglyceridemia—HSKO mice were generated by crossing ABCA1-floxed mice with albumin Cre transgenic mice as described previously (1). To determine the potential effect of hepatocyte ABCA1 expression on plasma TG concentrations, both fasted and non-fasted mice were studied. There

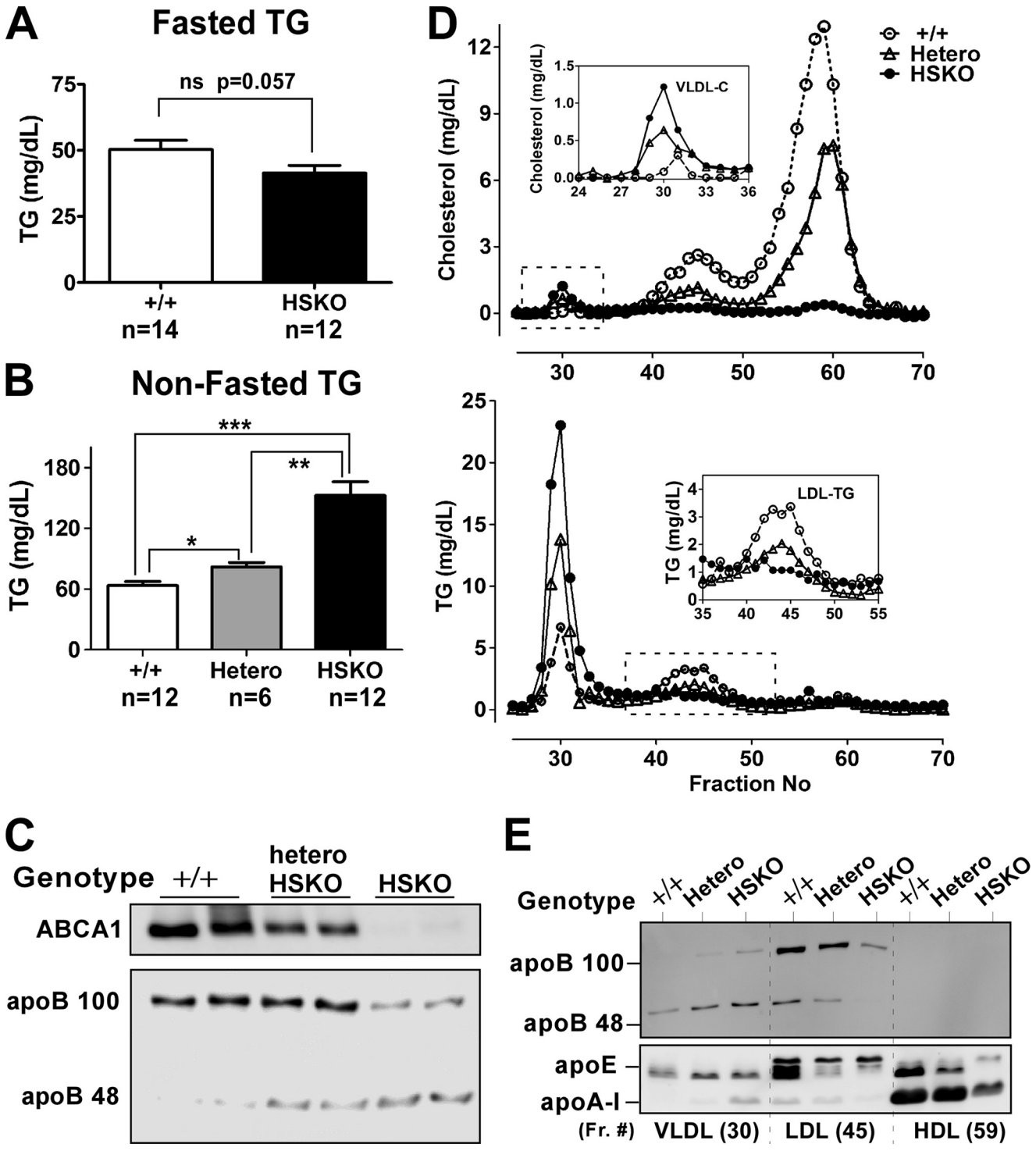

FIGURE 1. **Targeted deletion of hepatocyte ABCA1 induces hypertriglyceridemia.** Plasma was collected from fasted (*A*) and non-fasted (*B–E*) wild type (+/+), heterozygous (*Hetero*), and homozygous HSKO mice. *A*, fasted (6 h) plasma TG concentrations, mean ± S.E. *ns*, not significant. *B*, non-fasted plasma TG concentrations, mean ± S.E. *, $p < 0.05$; **, $p < 0.01$; ***, $p < 0.001$. *C*, Western blot analysis of hepatic ABCA1 expression and plasma levels of apoB100 and apoB48. Twenty μl of plasma were immunoprecipitated with anti-human apoB antibody, and the immunoprecipitates were fractionated by SDS-PAGE and Western blotted using the same anti-human apoB antibody. *D*, FPLC profiles of cholesterol (*top*) and triglyceride (*bottom*) in pooled plasma (450 μl; $n = 6$/genotype). *Insets* show the VLDL cholesterol (*top*) and LDL TG (*bottom*) results. *E*, Western blot analysis of 25 μl of selected FPLC fractions corresponding to *D*.

was no significant difference in TG levels in fasting WT and HSKO mice (Fig. 1*A*); however, in the non-fasting state, there was a significant elevation in plasma TG concentrations with successive deletion of hepatic ABCA1 alleles (63 ± 4, 82 ± 4, and 152 ± 13 mg/dl for WT, heterozygous, and homozygous HSKO, respectively) (Fig. 1*B*). Plasma apoB48 levels also demonstrated a stepwise increase with loss of hepatic ABCA1 expression, whereas apoB100 levels displayed a decrease in abundance that was particularly dramatic in homozygous HSKO mice (Fig. 1*C*). To further characterize the lipoprotein

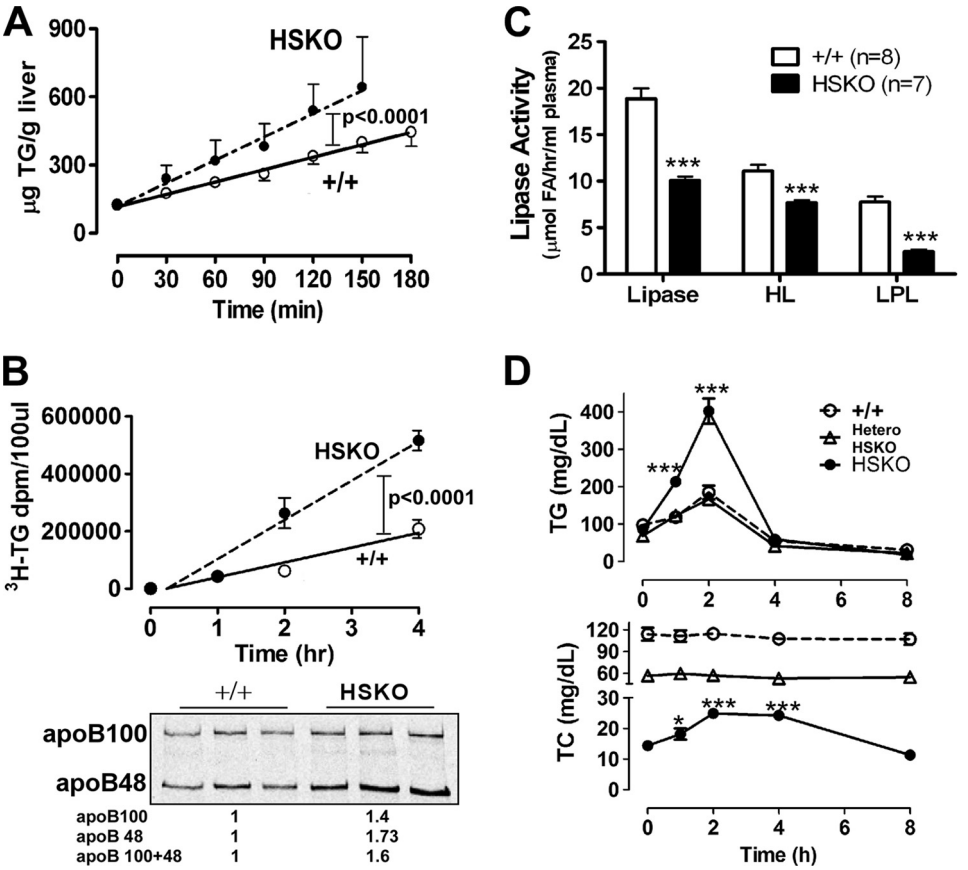

FIGURE 2. **Selective deletion of hepatocyte ABCA1 increases hepatic TG secretion and reduces post-heparin lipase activity.** *A*, TG mass accumulation per g of liver during isolated recirculating liver perfusion of WT (+/+) ($n = 6$) and HSKO ($n = 5$) mice. Data points denote mean TG ± S.E. of mice of the indicated genotype at each time point; the line of best fit, determined by linear regression analysis, is shown for both genotypes. Accumulation rates (μg/g liver/min) of TG were derived by linear regression analysis of the slope of the plot for each mouse. The mean ± S.E. accumulation rate was 1.87 ± 0.07 and 3.40 ± 0.20 μg/min/g liver for WT and HSKO mice, respectively. *B*, appearance of newly synthesized plasma TG and apoB after detergent block ($n = 3$ for each genotype). Data points denote the mean ± S.E. of radiolabeled TG in 100 μl of plasma; the line of best fit, determined by linear regression analysis, is shown for both genotypes. Accumulation rates were derived by linear regression analysis of the slope of the plot for each mouse; mean ± S.E. accumulation rates ([^{3}H]TG/100 μl of plasma/h) of TG were 51,550 ± 6,205 and 136,500 ± 12,480 for WT and HSKO mice, respectively. Accumulation of newly synthesized and secreted plasma apoB in the terminal plasma sample was determined after immunoprecipitation with anti-apoB antiserum, SDS-PAGE separation of proteins, and PhosphorImager analysis. Relative PhosphorImager intensity of total apoB (apoB100 + B48), normalized to a WT mouse sample, is shown *below* the gel. *C*, plasma isolated 15 min after intravenous heparin injection (300 units/kg) was used to measure the HL and LPL activity in WT (+/+, $n = 8$) and HSKO ($n = 7$) mice. *D*, plasma TG and TC concentration after oral gavage of olive oil (150 μl) in WT (+/+) and HSKO mice ($n = 4$/group). Data expressed in mean ± S.E. *, $p < 0.05$; ***, $p < 0.001$ by Student's *t* test.

response in non-fasted mice, pooled plasma was fractionated by FPLC. In addition to a striking reduction of HDL cholesterol as described previously (1), loss of hepatic *ABCA1* gene function caused a dose-dependent decrease in LDL cholesterol and LDL TG and an increase in VLDL cholesterol and VLDL TG (Fig. 1*D*). Western blot analysis of FPLC fractions corresponding to the major lipoprotein classes (Fig. 1*E*) revealed that hepatic inactivation of ABCA1 caused a gene dose-dependent increase in apoB48 and -100 in VLDL but a decrease in LDL. Thus, the whole plasma Western blot results in Fig. 1*C* can be explained by the increase of plasma apoB in VLDL and the decrease in LDL that occurs in HSKO mice relative to WT mice. It was also notable that inactivation of ABCA1 reduced apoE in the LDL and HDL fractions. As expected, apoA-I in HDL was reduced in the HSKO mice (Fig. 1*E*). Collectively, these data demonstrate that hepatocyte-specific inactivation of ABCA1 induces postprandial hypertriglyceridemia, characterized by an increase in plasma VLDL and a decrease in plasma LDL, recapitulating the TD lipid phenotype (10, 24).

Deletion of Hepatocyte ABCA1 Increases Hepatic TG Secretion and Reduces Post-heparin Plasma Lipolytic Activity—To determine whether hepatic production of TG contributes to the elevated levels of plasma TG in HSKO mice, we performed two studies. First, we measured hepatic TG mass secretion using isolated recirculating liver perfusion. The TG accumulation rate in liver perfusate of HSKO mice was twice that of WT mice (3.40 ± 0.20 *versus* 1.87 ± 0.07 μg/g liver/min; $p < 0.001$), suggesting hepatic TG mass secretion is increased in the absence of ABCA1 (Fig. 2*A*). In the second experiment, TG and apoB production were measured *in vivo* in the presence of the detergent poloxamer 407, to block TG lipolysis. Radiolabeled precursors ([^{3}H]oleic acid and [^{35}S]Met/Cys) were injected with the detergent, and the appearance of newly synthesized and secreted TG and apoB was monitored. In agreement with the liver perfusion data, the rate of TG secretion was 2.6-fold higher in HSKO mice relative to WT mice (Fig. 2*B*, *top*). Analysis of total radiolabeled apoB in the terminal plasma sample showed a 1.6-fold increase (1.4-fold in apoB100 and 1.73-fold in apoB48) in HSKO *versus* WT mice (Fig. 2*B*, *bottom*). Collectively, these data suggest that deficiency of hepatic ABCA1 expression increases hepatic TG secretion.

To determine whether reduced plasma lipolytic activity also contributed to the elevation of plasma TG in HSKO mice, HL and LPL activity were measured in post-heparin plasma using [^{3}H]triolein micelles as substrates. HSKO mice displayed a 50% reduction in total lipase activity relative to WT mice (18.86 ± 1.10 *versus* 10.10 ± 0.40 μmol of fatty acid released/h/ml of plasma), which was due to a ~30% reduction in HL activity (11.10 ± 0.64 *versus* 7.69 ± 0.28) and a ~70% reduction in LPL activity (7.76 ± 0.58 *versus* 2.4 ± 0.25) (Fig. 2*C*). In agreement with the reduced lipase activity, HSKO mice displayed delayed clearance of an oral fat load compared with WT mice (Fig. 2*D*). TPC during the oral fat load was constant for heterozygote and WT mice but showed a slight increase in HSKO mice, presumably due to the delayed clearance of chylomicron remnants and

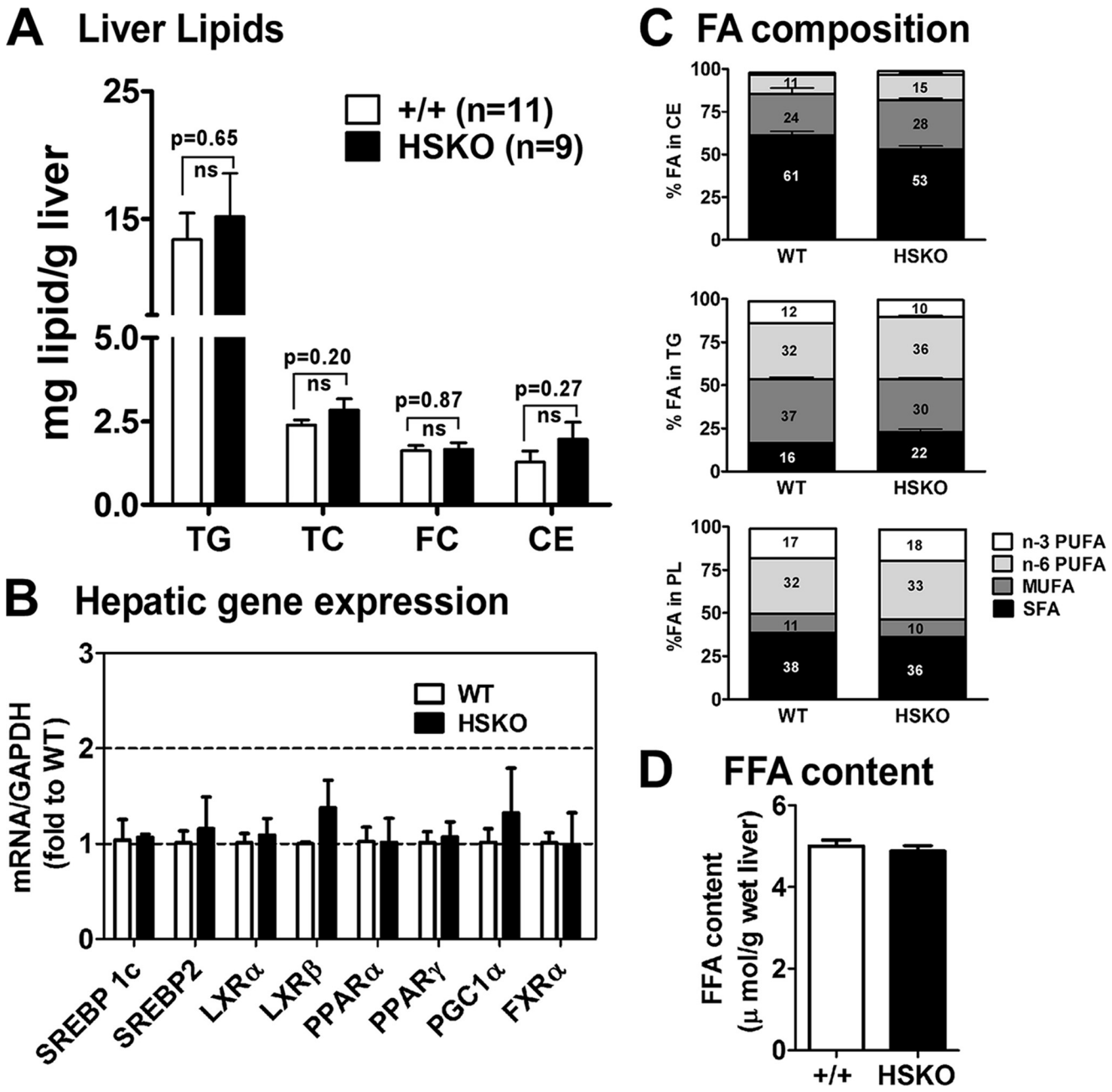

FIGURE 3. **Targeted deletion of hepatocyte ABCA1 does not alter liver lipid content, gene expression, or lipid fatty acid composition.** *A*, liver lipid content (TG, TC, free cholesterol (*FC*), and cholesteryl ester (*CE*)) in chow-fed wild type (+/+, $n = 11$) and HSKO ($n = 9$) mice was analyzed by enzymatic assays, and results were normalized to liver wet weight. *B*, mRNA expression of genes related to lipid metabolism were analyzed by quantitative real-time PCR and normalized to GAPDH expression. Mean ± S.E., $n = 6$/genotype. *C*, fatty acid (*FA*) composition of hepatic cholesteryl ester, TG, and phospholipid (*PL*) from wild type (+/+, $n = 3$) and HSKO (+/+, $n = 3$) mice was determined by gas-liquid chromatography. Percentage distribution of polyunsaturated fatty acids (*PUFA*; *n*-3 and *n*-6), monounsaturated fatty acids (*MUFA*), and saturated fatty acids (*SFA*) is shown in each *column*. *D*, hepatic free fatty acid (*FFA*) content was determined in liver from wild type and HSKO mice ($n = 5$/group) by enzymatic assay. Data are expressed as mean ± S.E. *ns*, not significant at $p = 0.05$ by Student's *t* test.

the low basal cholesterol concentrations in HSKO mouse plasma. Taken together, these data suggest that, in addition to effects on TG secretion, hepatic ABCA1 deficiency also affects the clearance of apoB lipoproteins.

To address whether hepatic deletion of ABCA1 altered hepatic lipid homeostasis, liver lipid content was analyzed. Total cholesterol (2.39 ± 0.15 *versus* 2.84 ± 0.3 μg/mg liver, $p = 0.20$), free cholesterol (1.62 ± 0.15 *versus* 1.66 ± 0.15 μg/mg liver, $p = 0.87$), and TG content (13.41 ± 2.02 *versus* 15.17 ± 3.45 μg/mg liver, $p = 0.65$) were similar for WT *versus* HSKO mice, respectively (Fig. 3*A*). Expression of hepatic lipid metabolism-related genes (Fig. 3*B*), fatty acid composition of liver lipids (Fig. 3*C*), and total free fatty acid content (Fig. 3*D*) were similar between the two genotypes of mice. Together, these data indicate that, despite alterations in TG secretion and lipolytic activity associated with inactivation of hepatic ABCA1, no major changes occurred in hepatic lipid content.

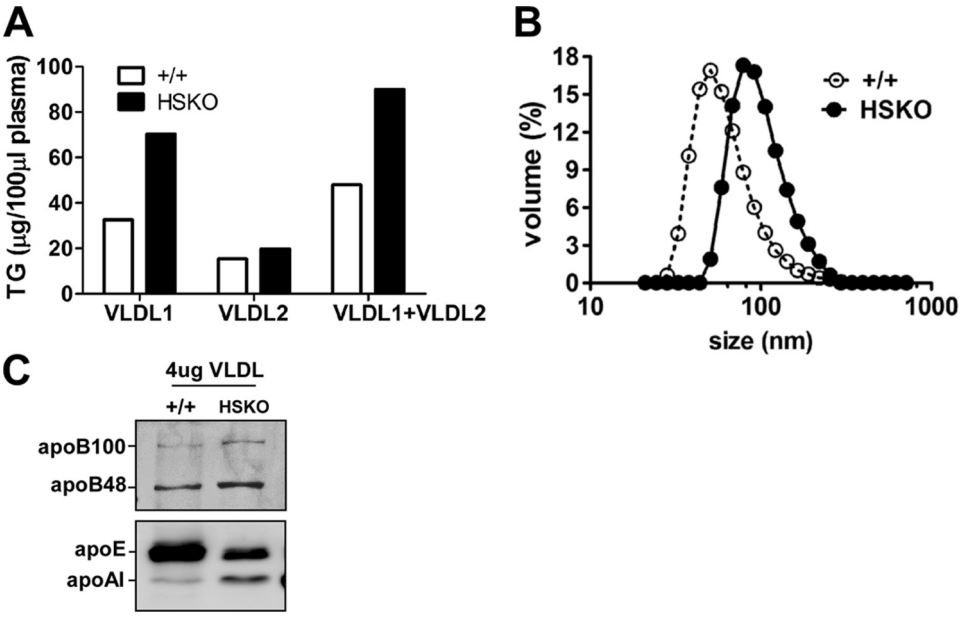

FIGURE 4. **Targeted deletion of hepatocyte ABCA1 increases plasma VLDL size.** *A*, fractionation of VLDL1 (S_f = 100–400) and VLDL2 (S_f = 20–100) in pooled plasma (n = 3/genotype, 200 μl total) by density gradient ultracentrifugation. VLDL1 and -2 were then assayed for TG concentration. *B*, VLDL size determination of pooled VLDL1 and VLDL2 fractions (equal volumes) by dynamic laser light scattering. *C*, VLDL fractions from *A* were concentrated, and 4 μg of VLDL protein was separated by 4–16% SDS-PAGE and transferred to polyvinylidene difluoride membrane for Western blot analysis of apoB, apoE, and apoA-I.

Loss of Hepatocyte ABCA1 Expression Increases Nascent VLDL Size and Attenuates PI3K Signaling—Overproduction of VLDL TG occurs in diabetes and metabolic syndrome and is associated with an increase in VLDL particle size (25, 26). To determine whether increased hepatic TG secretion in HSKO mice is associated with secretion of larger, more buoyant VLDL, pooled plasma (n = 3) was fractionated by density gradient ultracentrifugation into VLDL1 (S_f = 100–400) and VLDL2 (S_f = 20–100). As anticipated, there was a significant increase of VLDL1-TG in HSKO mice relative to WT mice, suggesting secretion of larger VLDL particles (Fig. 4*A*). In support of this result, VLDL size (measured by dynamic laser light scattering) was larger in HSKO (79.1 ± 0.4 nm) compared with WT mice (42.5 ± 3.1 nm) (Fig. 4*B*). Examination of VLDL (VLDL1 and -2) apolipoprotein content by Western blot analysis using an equivalent amount of VLDL protein (4 μg) revealed that VLDL from HSKO mice had more apoB48, apoB100, and apoA-I and less apoE (apoE/apoB ratio = 0.49 relative to WT) compared with WT mouse VLDL (Fig. 4*C*).

Previously, we showed that silencing of ABCA1 in rat hepatoma cells was associated with elevated TG secretion, increased VLDL particle size, and reduced PI3K activation (12). To examine whether PI3K activation was diminished in livers of HSKO mice, we stimulated the PI3K pathway by acute insulin administration or by subjecting mice to a fasting/refeeding protocol. Portal vein injection of insulin (5 units/kg) induced robust phosphorylation of PI3K p85 in WT liver, whereas there was a 28% decrease in HSKO liver (Fig. 5*A*; WT *versus* HSKO was 1 *versus* 0.72 ± 0.008; n = 3 mice/treatment, p = 0.031). In the fasting/re-feeding experiments, PI3K phosphorylation was reduced 31% in HSKO compared with WT liver (Fig. 5*B*; 1 *versus* 0.72 ± 0.004; n = 3 mice per treatment, p = 0.01), and Akt phosphorylation was 63% lower (1 *versus* 0.36 ± 0.059; n = 3 mice/treatment, p = 0.038). Moreover, *in vivo* pharmacological inhibition of PI3K by wortmannin, prior to detergent blockage of lipolysis, had little effect on plasma TG and secretion of newly synthesized apoB in HSKO mice (Fig. 5*C*, *HSKO* ± *Wort*). On the other hand, *in vivo* inhibition of PI3K activation with wortmannin in WT mice resulted in increased plasma TG as well as apoB secretion (+/+; compare ± *Wort*), to levels similar to those observed in HSKO mice (Fig. 5*C*). Effects of PI3K activation on hepatic TG secretion was also investigated in primary hepatocytes. Synthesis and secretion of TG from [^{3}H]oleate was almost 3-fold higher in HSKO mice (Fig. 5*D*). Consistent with *in vivo* results, phosphorylation of PI3K p85 was diminished in primary hepatocytes from HSKO mice as compared with WT mice (Fig. 5*D*). However, hepatic microsomal transfer protein (MTP) mRNA and protein levels were similar (Fig. 5*E*), suggesting that up-regulation of MTP is not the basis for increased TG secretion caused by hepatic ABCA1 deficiency. These data provide mechanistic evidence that targeted inactivation of hepatic ABCA1 attenuates activation of PI3K, which in turn, contributes to increased secretion of larger TG-enriched VLDL.

Selective Hepatocyte ABCA1 Deletion Increases Plasma Clearance of LDL—To determine whether loss of hepatic ABCA1 expression contributes to reduced plasma LDL concentrations by increasing LDL clearance from plasma, we performed turnover studies using LDL isolated from LDLrKO mice. Isolated LDL was radioiodinated with ^{125}I and intravenously injected into WT and HSKO recipient mice, after which plasma clearance of the ^{125}I-LDL tracer was measured. The LDL tracer was removed from plasma more rapidly in HSKO recipient mice compared with WT mice (Fig. 6*A*). The FCR (pools/day) of ^{125}I-LDL apoB was significantly ($p < 0.001$) higher in HSKO mice than WT mice (5.26 ± 0.28 *versus* 2.95 ± 0.15) (Fig. 6*A*). Surprisingly, hepatic LDLr mRNA (Fig. 6*B*) and protein (Fig. 6*C*) abundance were markedly increased in the absence of hepatic ABCA1, suggesting that hepatic LDLr-mediated clearance contributed to the higher LDL FCR observed in HSKO mice.

To further explore this hypothesis, we crossed HSKO mice with LDLrKO mice. In the LDLrKO background, there was still a significant elevation in plasma TG concentrations associated with successive deletion of hepatic ABCA1 alleles (60.7 ± 2.0, 69 ± 3.9, 93.8 ± 7.0 mg/dl for WT, heterozygous, homozygous HSKO in LDLrKO background; Fig. 6*D*, *top*), similar to the plasma TG response trend of mice with functional LDL receptors (Fig. 1*B*). Although total plasma cholesterol was significantly lower in HSKO mice in the LDLrKO background

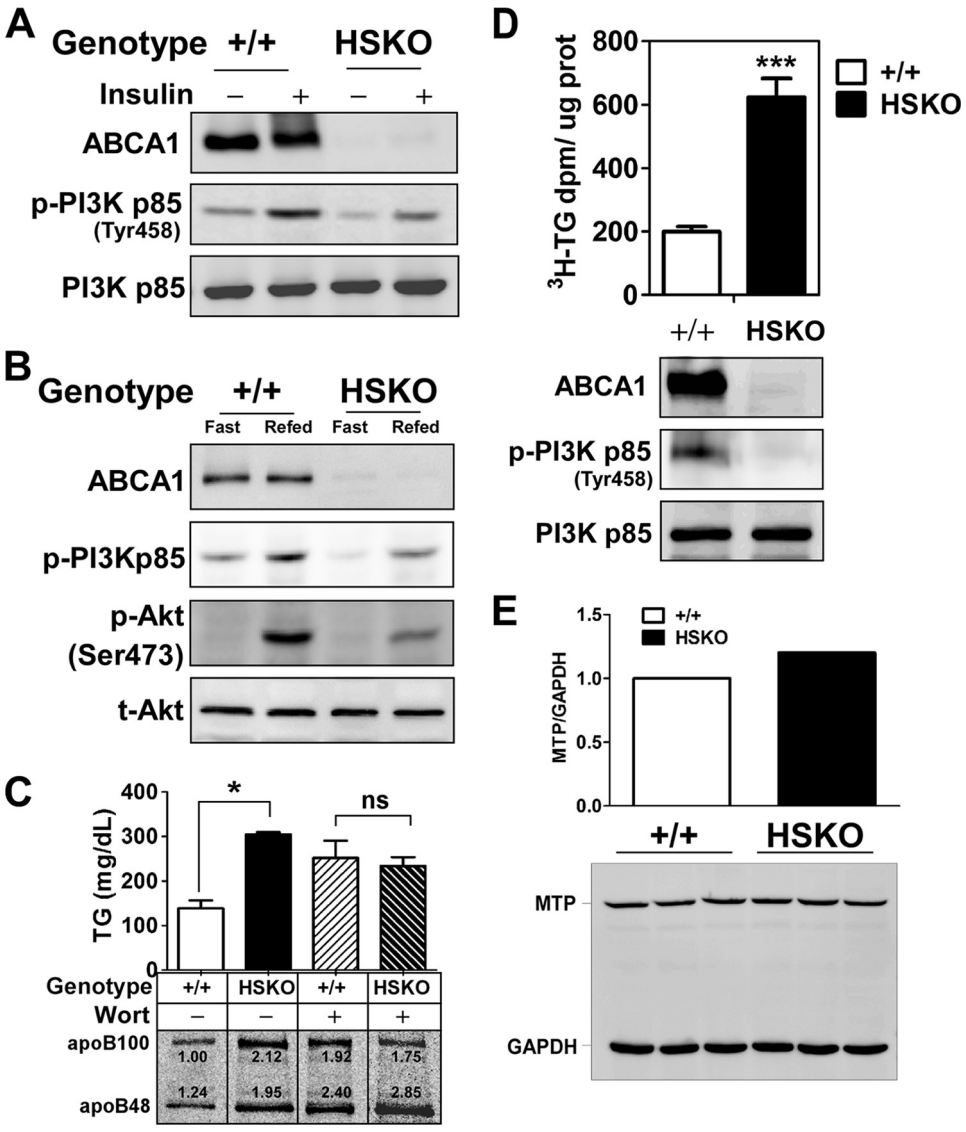

FIGURE 5. **Targeted deletion of hepatocyte ABCA1 induces defective PI3K signaling.** *A*, Western blot analysis of liver ABCA1, PI3K p85, and phospho-PI3K p85 expression 5 min after insulin (5 units/kg) injection into the portal vein. *B*, Western blot analysis of liver phospho-PI3K p85 (*p-PI3Kp85*), phospho-Akt (*p-Akt*), and total Akt (*t-Akt*) expression after fasting or fasting/refeeding of mice. *C*, PI3K inhibitor, wortmannin (1.5 μg/g body weight in DMSO), or DMSO alone was injected into the peritoneal cavity of mice 1 h prior to injection of detergent (1000 mg of poloxamer 407/kg of body weight) to block lipolysis and 7 μCi of [^{35}S]Cys/Met/g of body weight as described under "Experimental Procedures." Plasma TG concentration (mean ± S.E., $n = 3$) and apoB phosphor image (*bottom*) were analyzed 2 h after detergent block. Relative PhosphorImager intensity of apoB is shown *below* each *lane*. Values were normalized to the apoB100 band in the DMSO-treated WT mouse. *D*, triglyceride secretion ([^{3}H]TG) and PI3K phosphorylation from isolated primary hepatocytes. *E*, quantification of MTP expression in livers of WT and HSKO mice by real-time PCR (mRNA pool from 3 mice/genotype; *top*) and Western blot analysis ($n = 3$ of each genotype; *bottom*). Data were normalized to GAPDH expression. Data are expressed as mean ± S.E. *, $p < 0.05$; ***, $p < 0.001$ by Student's *t* test. *ns*, not significant.

(Fig. 6*D*, *bottom*), this was due to exclusively to a marked decrease in HDL cholesterol (46 *versus* 8 mg/dl in LDLrKO *versus* LDLrKO, HSKO mice; Fig. 6*F*). However, in contrast to LDL-replete mice (Fig. 1*D*), LDL cholesterol concentrations were similar (106 *versus* 103 mg/dl in LDLrKO *versus* LDLrKO, HSKO mice) (Fig. 6*F*), suggesting that hepatic LDLr-mediated clearance is the major cause for reduced LDL concentrations in HSKO mice. There was also a decrease in scavenger receptor B-I and endothelial lipase expression in HSKO liver (supplemental Fig. 1). In summary, the significantly lower plasma LDL concentrations in HSKO mice appear to be due to more rapid plasma clearance of LDL particles, secondary to increased hepatic LDLr expression.

Adenoviral Repletion of ABCA1 Normalizes Plasma TG Concentrations in High Fat-fed HSKO Mice—To determine whether repletion of hepatic ABCA1 would reverse the plasma lipid phenotype of HSKO mice, we injected intravenously Ad-ABCA1 or Ad-AP (control) into WT and HSKO mice fed an HF diet for 8 weeks. The HF diet was employed to more closely mimic the human dietary situation and to increase plasma and liver lipid concentrations. Three days after injection, Ad-ABCA1 had restored ~60% of WT hepatic ABCA1 expression in HSKO mice, whereas it induced a 2-fold increase in hepatic ABCA1 levels in WT mice (Fig. 7*A*; the anti-ABCA1 antibody was raised using a peptide whose sequence is identical between mouse and human ABCA1). Consistent with data generated using chow-fed mice (Fig. 6*C*), hepatic LDLr protein expression was also higher in HF-fed HSKO mice compared with WT mice; however, in neither background did short term overexpression strongly impact hepatic LDLr expression. Moreover, similar to results in chow-fed mice (Fig. 5, *A* and *B*), PI3K phosphorylation was reduced in HF-fed HSKO mice; however, partial repletion of hepatic ABCA1 in HSKO by adenoviral delivery of human ABCA1 restored PI3K phosphorylation to a level comparable with levels in Ad-ABCA1-treated WT liver (Fig. 7*A*). TPC was significantly increased in WT mice injected with Ad-ABCA1 compared with Ad-AP (Fig. 7*B*; 251 ± 23 *versus* 154 ± 3 mg/dl; $n = 4$) due to increases in LDL and HDL cholesterol (Fig. 7*C*). In HSKO mice, Ad-ABCA1 expression actually decreased TPC concentration (Fig. 7*B*) by decreasing VLDL cholesterol concentration to a greater extent than it increased HDL cholesterol (Fig. 7*D*). Plasma TG concentration was unchanged in WT mice injected with Ad-ABCA1 *versus* Ad-AP (Fig. 7*B*) due to an increase in VLDL TG and a reciprocal decrease in LDL TG (Fig. 7*E*). In HSKO mice, Ad-ABCA1 injection resulted in a normalization of plasma TG concentration to WT levels (Fig. 7*B*) and a striking decrease in

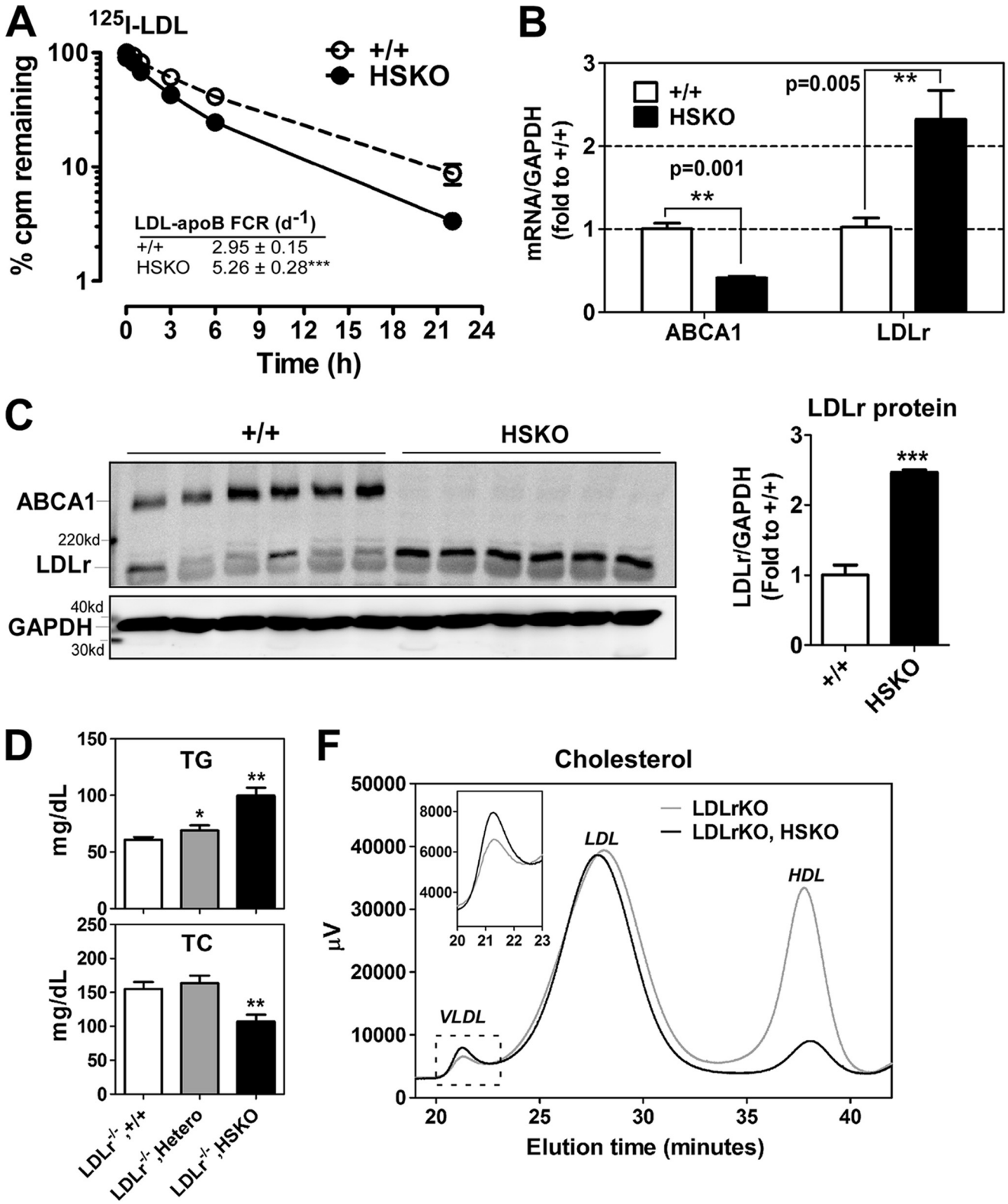

FIGURE 6. **Hepatocyte-specific deletion of ABCA1 induces rapid LDL clearance from plasma.** LDL from LDLrKO mice was isolated and radioiodinated with ^{125}I. *A*, ^{125}I-LDL tracer was injected into WT and HSKO recipient mice, and periodic blood samples were taken to quantify the amount of tracer remaining in plasma (results normalized to the 2 min time point). Mean ± S.E., $n = 4$. FCR values (mean ± S.E.) were calculated from individual plasma die-away curves using a biexponential curve-fitting program. ***, $p < 0.001$ by Student's *t* test. *B*, real-time PCR quantification of hepatic ABCA1 and LDLr mRNA levels. Data were normalized to GAPDH expression (mean ± S.E.; $n = 6$). *C*, liver protein (50 μg) from WT and HSKO mice was fractionated by SDS-PAGE and analyzed for expression of ABCA1, LDLr, and GAPDH by Western blot. Relative quantification of the blot is shown on the *right*. Data are expressed as mean ± S.E. *D*, effects of hepatic ABCA1 deficiency on non-fasting plasma TG (*top*) and TC (*bottom*) in the LDLrKO background. Shown are wild type (LDLrKO, +/+), heterozygous (LDLrKO, *Hetero*), and homozygous HSKO (LDLrKO, *HSKO*) mice ($n = 4$/group), mean ± S.E. *F*, FPLC-cholesterol profiles of pooled plasma of wild type (LDLrKO, +/+) and HSKO (LDLrKO, *HSKO*) mice in the LDLrKO background ($n = 4$/group). *Inset*, expanded VLDL region. *, $p < 0.05$; **, $p < 0.01$; ***, $p < 0.001$ by Student's *t* test (*A* and *B*) or analysis of variance (*D*).

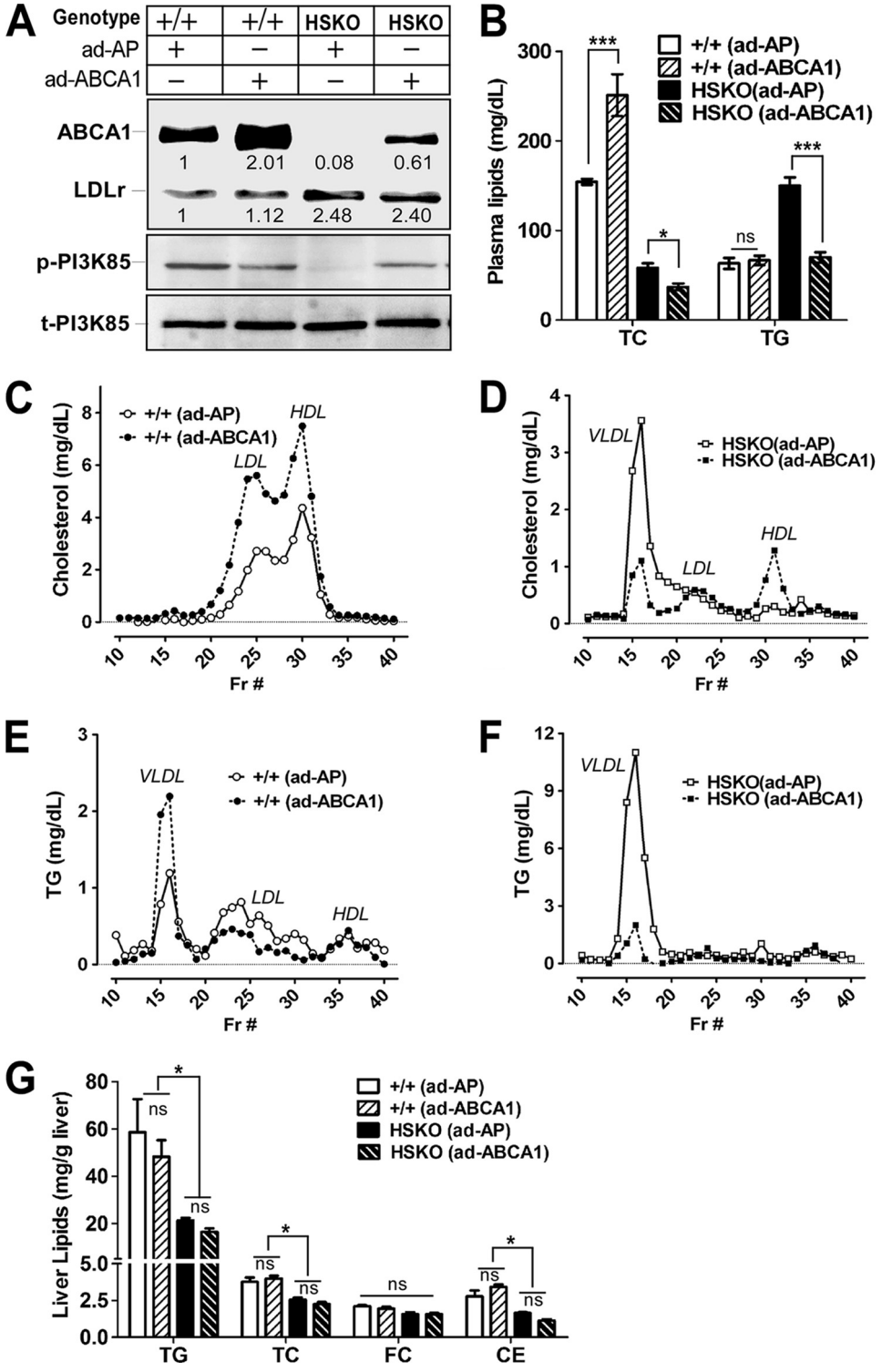

FIGURE 7. **Adenoviral overexpression of ABCA1 normalizes plasma TG concentrations in HSKO mice.** Mice were fed an HF diet for 8 weeks before intravenous injection of either Ad-AP or Ad-ABCA1. Mice were sacrificed 3 days later to collect liver and plasma samples. *A*, Western blot analysis of hepatic ABCA1, LDLr, phosphorylated PI3K (*p-PI3K*), and total PI3K (*t-PI3K*) expression in wild type (WT; +/+) and HSKO mice. ABCA1 and LDLr expression level were quantified (normalized to GAPDH). Expression relative to control mice is denoted *below* each band. *B*, plasma concentrations of TG and TC in WT and HSKO mice ($n = 4$/group) after adenovirus injection. Data are expressed as mean ± S.E. *, $p < 0.05$; ***, $p < 0.001$ by Student's *t* test. *C*, FPLC-cholesterol profile from pooled plasma of WT mice ($n = 4$) after adenoviral administration. *D*, FPCL-cholesterol profile from pooled plasma of HSKO mice ($n = 4$) after adenovirus administration. *E*, FPLC-TG profile from pooled plasma of WT mice ($n = 4$) after adenovirus administration. *F*, FPLC-TG profile from pooled plasma of HSKO mice ($n = 4$) after adenovirus administration. *G*, hepatic content of TG, TC, FC, and cholesteryl ester (*CE*) in WT and HSKO mice ($n = 4$/group). Data are expressed as mean ± S.E. *, $p < 0.05$ by one-way analysis of variance with Tukey's multiple comparison.

VLDL TG (Fig. 7*F*). Because plasma lipase activity was unchanged over the relatively short time course of the adenovirus experiment (data not shown), it is likely that the decreased plasma TG levels in HSKO mice treated with Ad-ABCA1 was due to decreased hepatic TG secretion, not increased TG hydrolysis. Unlike the situation in chow-fed mice in which hepatic liver lipid content was similar between WT and HSKO mice (Fig. 3*A*), HF-fed HSKO mice displayed a paradoxical decrease in hepatic TG and TC content relative to WT mice (Fig. 7*G*), and acute repletion of hepatic ABCA1 did not affect hepatic lipid content in either genotype of mice. These results demonstrate that acute, partial (60%) repletion of hepatic ABCA1 expression in HSKO mice can normalize plasma TG concentrations within 3 days, although HDL cholesterol concentrations were not fully recovered to WT levels.

DISCUSSION

It is well established that ABCA1 influences HDL metabolism in humans, mice, and chickens (27); however, its role in metabolism of apoB-containing lipoproteins remains elusive. In the present study, we demonstrated that targeted inactivation of ABCA1 in hepatocytes recapitulates the lipid phenotype of TD subjects, including reduced HDL and LDL cholesterol, and elevated TG concentrations. We established that part of the lipid phenotype associated with hepatic ABCA1 deficiency results from an increased secretion of TG-enriched hepatic VLDL via a PI3K-dependent pathway. We also documented decreased post-heparin lipolytic activity and increased hepatic LDLr expression, resulting in a net increase in clearance of LDL from the circulation. Furthermore, elevated plasma VLDL TG was rescued by adenoviral expression of human ABCA1, demonstrating the existence of a coupled regulatory pathway between HDL and apoB Lps through hepatic ABCA1. The com-

bined results suggest that, in addition to its well recognized role in HDL biogenesis, hepatic ABCA1 plays a significant and complex role in apoB LP metabolism.

Previously, we reported that silencing of ABCA1 in rat hepatoma cells decreased formation of large (>10-nm diameter) nascent HDL particles, increased secretion of large, buoyant TG-enriched VLDL, and attenuated PI3K activation (12). We further demonstrated that the addition of nascent HDL particles, the product of ABCA1-mediated lipidation of apoA-I, to ABCA1-silenced hepatoma cells reversed the blockage of PI3K activation and restored the basal rate of TG secretion. The present study demonstrates the physiological relevance of our previous *in vitro* observations using rat hepatoma cells and suggests a new mechanism for the elevated plasma TG concentrations associated with TD. We show that selective hepatic ABCA1 deficiency in mice increases hepatic VLDL TG secretion *ex vivo*, using isolated liver perfusion (Fig. 2*A*) and cultured primary hepatocytes (Fig. 5*D*), and *in vivo*, using detergent to block VLDL catabolism (Fig. 2*B*). Furthermore, as assessed by both differential ultracentrifugation and dynamic laser light scatter data, hepatic ABCA1 deficiency resulted in the formation of larger, TG-enriched VLDL particles (Fig. 4, *A* and *B*), similar to our previous findings with rat hepatoma cells (12). Finally, acute, partial repletion of hepatic ABCA1 expression with adenovirus resulted in normalization of plasma VLDL TG concentration (Fig. 7, *B* and *F*). These results collectively suggest a mechanistic link between nascent HDL formed by ABCA1 and hepatic VLDL TG secretion.

The mechanism responsible for ABCA1-mediated regulation of VLDL assembly and secretion appears to involve a PI3K-dependent pathway based on multiple lines of evidence. First, HSKO mice demonstrated attenuated phosphorylation of hepatic PI3K p85 and its downstream target, Akt, in response to both acute injection of insulin- and glucose-stimulated endogenous insulin release (*i.e.* fasting-refeeding; Fig. 5, *A* and *B*). Second, diminished PI3K activation was observed in cultured primary hepatocytes from HSKO mice in conjunction with increased TG secretion (Fig. 5*D*). Third, plasma TG concentrations of WT mice were elevated to levels similar to those of HSKO mice after acute *in vivo* inhibition of PI3K with wortmannin (Fig. 5*C*). Finally, partial adenoviral repletion of hepatic ABCA1 rescued PI3K activation and normalized plasma TG concentrations (Fig. 7, *A* and *F*). These results, along with our previous *in vitro* data (12), firmly establish a mechanistic link through which hepatic ABCA1 expression regulates hepatic PI3K activity, hepatic TG secretion, and plasma TG concentration.

The relationship between VLDL particle assembly and PI3K has been noted previously and, in part, underlies the ability of insulin to acutely regulate hepatic VLDL TG output (28–30). The interface between PI3K-dependent signaling and apoB assembly and secretion is not known in detail, although in some studies, insulin-mediated signaling, via PI3K and Akt, regulates MTP expression and, hence, VLDL particle number and size (18, 29, 31, 32). Although MTP is the target for some forms of PI3K-mediated regulation of VLDL assembly (32), MTP expression was unaffected by ABCA1 deficiency in this study (Fig. 4*E*) or by silencing of ABCA1 in rat hepatoma cells in our previous study (12), suggesting that other mechanisms are operational.

VLDL particle assembly occurs in two steps: the co-translational lipidation of apoB by MTP to form a small, dense apoB-containing pre-VLDL, followed by a pre-VLDL particle fusion with TG lipid droplets in the secretory pathway to form mature VLDL particles (33, 34). Several studies have indicated that the insulin/PI3K effects on VLDL production occur during the second, pre-VLDL enlargement step of particle assembly (28, 30). The current studies demonstrate that VLDL from HSKO mice is more buoyant and of larger diameter than that of WT mice, which is also consistent with ABCA1/PI3K exerting effects during the second step of VLDL assembly. Because PI3K is present in the endoplasmic reticulum and Golgi, is involved in intracellular vesicular trafficking, and is increased with insulin stimulation (29, 35, 36), we hypothesize that the lack of ABCA1 in hepatocytes and the resultant attenuation of PI3K activation results in slower VLDL transit through the secretory pathway, allowing additional time for second step VLDL particle expansion. This hypothesis is supported by the observations of defective lipid and vesicular trafficking from the Golgi to the plasma membrane in fibroblasts from TD subjects (37–40).

Reduced LPL activity has also been suggested to explain the elevated TG levels in TD subjects. For example, Wang *et al.* (10) showed that VLDL from TD subjects was enriched with apoA-II and apoC-III, compared with VLDL from normolipidemic subjects, resulting in a reduced lipase accessibility. Consistent with this notion, Kyreos *et al.* (41) recently showed that adenoviral overexpression of human apoC-III in apoE KO and ABCA1 KO mice induces hypertriglyceridemia due to low LPL reactivity of apoC-III-enriched VLDL. In addition to possible effects on VLDL substrate, our mouse model also showed that both HL and LPL were markedly reduced upon deletion of hepatic ABCA1 (Fig. 2*C*). Therefore, it is likely that the decrease in HL and LPL in HSKO mice contributed, in large part, to the increase in plasma TG and apoB48 levels observed in the postprandial state (Figs. 1, *B* and *C*, and 2*D*). These findings may explain why elevated plasma TG levels in TD patients are more evident postprandially (9).

Despite elevated plasma TG concentrations, TD subjects have LDL concentrations that are reduced by ~40–50% (8). Schaefer *et al.* (42) demonstrated that this was due to a 2-fold increase in FCR of LDL. Supporting this finding, Zha *et al.* (43) reported enhanced uptake of LDL by fibroblasts from TD subjects that appeared related to increased endocytosis. Similar to TD subjects, HSKO mice demonstrated a 2-fold increased removal rate of LDL tracer from plasma compared with WT mice (Fig. 6*A*). The increased catabolism of LDL probably resulted from the 2.5-fold increase in expression (mRNA and protein) of hepatic LDLr (Fig. 6, *B* and *C*). The increase in hepatic LDLr expression in HSKO mice appears unrelated to hepatic sterol content, because chow-fed WT and HSKO mice had similar hepatic lipid content and expression of cholesterol-sensitive genes (supplemental Fig. 1*A*). Additional evidence to support our conclusion that increased hepatic LDLr expression is responsible for the decreased plasma LDL concentrations in HSKO mice comes from our studies in which HSKO mice were crossed into the LDLrKO background. In the absence of whole-

body LDLr expression, we observed similar plasma LDL concentrations in LDLrKO and HSKO-LDLrKO mice (Fig. 6*F*), although plasma TG concentrations were still significantly higher in HSKO-LDLrKO mice relative to LDLrKO mice. These results suggest that two separate mechanisms, increased hepatic LDLr expression and increased hepatic TG secretion, are responsible for the reduced plasma LDL and increased plasma TG concentrations, observed under conditions of hepatic ABCA1 expression deficiency.

Transgenic LDLrKO mice with 2.3-fold overexpression of ABCA1 protein in the liver displayed significantly increased plasma VLDL, LDL, and HDL cholesterol concentrations, increased apoA-I and apoB levels, delayed clearance of VLDL and LDL tracers, and an increase in atherosclerosis (44). These data led to the hypothesis that liver ABCA1 may play a proatherogenic role *in vivo*, resulting from its dramatic effects on the metabolism of apoB-containing lipoproteins. These mice also displayed increased plasma TG concentrations, perhaps due to a small but significantly delayed clearance of plasma VLDL particles caused by their cholesterol enrichment. However, a more modest overexpression of ABCA1 protein (~25%) using the endogenous ABCA1 promoter in LDLrKO mice resulted in no significant increase in apoB-containing lipoprotein concentration and a significant reduction in atherosclerosis, probably due to an increase in macrophage ABCA1 protein expression (45). The reasons for the apparently discrepant impact of ABCA1 overexpression on LDL concentrations and atherosclerosis in LDLrKO mice are 2-fold. First, the regulatory elements controlling the sites and regulation of ABCA1 expression were different in the two studies. Second, the extent of ABCA1 overexpression was ~10-fold higher when the apoE promoter was used (~2.5-fold over expression) *versus* the endogenous ABCA1 promoter (0.25-fold increase). Indeed, when a 2.6-fold overexpression of ABCA1 was achieved in the liver using a cytomegalovirus promoter in adenovirus, significant increases in the concentration of plasma proatherogenic apoB-containing lipoproteins as well as HDL cholesterol were observed (22). Taken together, these studies complement our data and demonstrate that when hepatic ABCA1 is overexpressed to a sufficient extent, LDL concentrations are elevated, whereas liver-specific deletion of ABCA1 results in reduced plasma LDL concentrations.

In summary, our data support an important and emerging role for hepatic ABCA1 expression in the production and catabolism of apoB lipoproteins and suggest new mechanisms to account for the increased plasma TG and decreased LDL concentrations observed in TD subjects. Furthermore, the decreased LDL levels may explain why some TD subjects have only minimally increased risk of coronary heart disease despite having extremely low plasma HDL levels (4).

Acknowledgment—We gratefully acknowledge Karen Klein (Research Support Core, Wake Forest University Health Sciences) for editing the manuscript.

REFERENCES

1. Timmins, J. M., Lee, J. Y., Boudyguina, E., Kluckman, K. D., Brunham, L. R., Mulya, A., Gebre, A. K., Coutinho, J. M., Colvin, P. L., Smith, T. L., Hayden, M. R., Maeda, N., and Parks, J. S. (2005) *J. Clin. Invest.* **115,** 1333–1342
2. Brunham, L. R., Kruit, J. K., Iqbal, J., Fievet, C., Timmins, J. M., Pape, T. D., Coburn, B. A., Bissada, N., Staels, B., Groen, A. K., Hussain, M. M., Parks, J. S., Kuipers, F., and Hayden, M. R. (2006) *J. Clin. Invest.* **116,** 1052–1062
3. Wellington, C. L., Walker, E. K., Suarez, A., Kwok, A., Bissada, N., Singaraja, R., Yang, Y. Z., Zhang, L. H., James, E., Wilson, J. E., Francone, O., McManus, B. M., and Hayden, M. R. (2002) *Lab. Invest.* **82,** 273–283
4. Assman, G., von Eckardstein, A., and Brewer, H. B., Jr. (2001) in *The Metabolic and Molecular Bases of Inherited Disease* (Scriver, C. R., Beaudet, A. L., Sly, W. S., Valle, D., Childs, B., Kinzler, K. W., and Volkman, B. F., eds) pp. 2937–2960, McGraw-Hill, New York
5. Bodzioch, M., Orsó, E., Klucken, J., Langmann, T., Böttcher, A., Diederich, W., Drobnik, W., Barlage, S., Büchler, C., Porsch-Ozcürümez, M., Kaminski, W. E., Hahmann, H. W., Oette, K., Rothe, G., Aslanidis, C., Lackner, K. J., and Schmitz, G. (1999) *Nat. Genet.* **22,** 347–351
6. Brooks-Wilson, A., Marcil, M., Clee, S. M., Zhang, L. H., Roomp, K., van Dam, M., Yu, L., Brewer, C., Collins, J. A., Molhuizen, H. O., Loubser, O., Ouelette, B. F., Fichter, K., Ashbourne-Excoffon, K. J., Sensen, C. W., Scherer, S., Mott, S., Denis, M., Martindale, D., Frohlich, J., Morgan, K., Koop, B., Pimstone, S., Kastelein, J. J., Genest, J., Jr., and Hayden, M. R. (1999) *Nat. Genet.* **22,** 336–345
7. Rust, S., Rosier, M., Funke, H., Real, J., Amoura, Z., Piette, J. C., Deleuze, J. F., Brewer, H. B., Duverger, N., Denèfle, P., and Assmann, G. (1999) *Nat. Genet.* **22,** 352–355
8. Clee, S. M., Kastelein, J. J., van Dam, M., Marcil, M., Roomp, K., Zwarts, K. Y., Collins, J. A., Roelants, R., Tamasawa, N., Stulc, T., Suda, T., Ceska, R., Boucher, B., Rondeau, C., DeSouich, C., Brooks-Wilson, A., Molhuizen, H. O., Frohlich, J., Genest, J., Jr., and Hayden, M. R. (2000) *J. Clin. Invest.* **106,** 1263–1270
9. Kolovou, G., Daskalova, D., Anagnostopoulou, K., Hoursalas, I., Voudris, V., Mikhailidis, D. P., and Cokkinos, D. V. (2003) *J. Clin. Pathol.* **56,** 937–941
10. Wang, C. S., Alaupovic, P., Gregg, R. E., and Brewer, H. B., Jr. (1987) *Biochim. Biophys. Acta* **920,** 9–19
11. Sahoo, D., Trischuk, T. C., Chan, T., Drover, V. A., Ho, S., Chimini, G., Agellon, L. B., Agnihotri, R., Francis, G. A., and Lehner, R. (2004) *J. Lipid Res.* **45,** 1122–1131
12. Chung, S., Gebre, A. K., Seo, J., Shelness, G. S., and Parks, J. S. (2010) *J. Lipid Res.* **51,** 729–742
13. Furbee, J. W., Jr., Francone, O., and Parks, J. S. (2002) *J. Lipid Res.* **43,** 428–437
14. Carr, T. P., Andresen, C. J., and Rudel, L. L. (1993) *Clin. Biochem.* **26,** 39–42
15. Lee, R. G., Shah, R., Sawyer, J. K., Hamilton, R. L., Parks, J. S., and Rudel, L. L. (2005) *J. Lipid Res.* **46,** 1205–1212
16. Millar, J. S., Cromley, D. A., McCoy, M. G., Rader, D. J., and Billheimer, J. T. (2005) *J. Lipid Res.* **46,** 2023–2028
17. Yamada, N., and Havel, R. J. (1986) *J. Lipid Res.* **27,** 910–912
18. Chirieac, D. V., Davidson, N. O., Sparks, C. E., and Sparks, J. D. (2006) *Am. J. Physiol. Gastrointest. Liver Physiol.* **291,** G382–G388
19. Wilcox, R. W., Thuren, T., Sisson, P., Kucera, G. L., and Waite, M. (1991) *Lipids* **26,** 283–288
20. Parks, J. S., and Rudel, L. L. (1982) *J. Lipid Res.* **23,** 410–421
21. Singaraja, R. R., Van Eck, M., Bissada, N., Zimetti, F., Collins, H. L., Hildebrand, R. B., Hayden, A., Brunham, L. R., Kang, M. H., Fruchart, J. C., Van Berkel, T. J., Parks, J. S., Staels, B., Rothblat, G. H., Fiévet, C., and Hayden, M. R. (2006) *Circulation* **114,** 1301–1309
22. Wellington, C. L., Brunham, L. R., Zhou, S., Singaraja, R. R., Visscher, H., Gelfer, A., Ross, C., James, E., Liu, G., Huber, M. T., Yang, Y. Z., Parks, R. J., Groen, A., Fruchart-Najib, J., and Hayden, M. R. (2003) *J. Lipid Res.* **44,** 1470–1480
23. Zhu, X., Lee, J. Y., Timmins, J. M., Brown, J. M., Boudyguina, E., Mulya, A., Gebre, A. K., Willingham, M. C., Hiltbold, E. M., Mishra, N., Maeda, N., and Parks, J. S. (2008) *J. Biol. Chem.* **283,** 22930–22941
24. Serfaty-Lacrosniere, C., Civeira, F., Lanzberg, A., Isaia, P., Berg, J., Janus, E. D., Smith, M. P., Jr., Pritchard, P. H., Frohlich, J., and Lees, R. S. (1994) *Atherosclerosis* **107,** 85–98
25. Adiels, M., Borén, J., Caslake, M. J., Stewart, P., Soro, A., Westerbacka, J.,

Wennberg, B., Olofsson, S. O., Packard, C., and Taskinen, M. R. (2005) *Arterioscler. Thromb. Vasc. Biol.* **25,** 1697–1703
26. Adiels, M., Westerbacka, J., Soro-Paavonen, A., Häkkinen, A. M., Vehkavaara, S., Caslake, M. J., Packard, C., Olofsson, S. O., Yki-Järvinen, H., Taskinen, M. R., and Borén, J. (2007) *Diabetologia* **50,** 2356–2365
27. Attie, A. D., Kastelein, J. P., and Hayden, M. R. (2001) *J. Lipid Res.* **42,** 1717–1726
28. Brown, A. M., and Gibbons, G. F. (2001) *Arterioscler. Thromb. Vasc. Biol.* **21,** 1656–1661
29. Phung, T. L., Roncone, A., Jensen, K. L., Sparks, C. E., and Sparks, J. D. (1997) *J. Biol. Chem.* **272,** 30693–30702
30. Sparks, J. D., Phung, T. L., Bolognino, M., and Sparks, C. E. (1996) *Biochem. J.* **313,** 567–574
31. Au, C. S., Wagner, A., Chong, T., Qiu, W., Sparks, J. D., and Adeli, K. (2004) *Metabolism* **53,** 228–235
32. Kamagate, A., Qu, S., Perdomo, G., Su, D., Kim, D. H., Slusher, S., Meseck, M., and Dong, H. H. (2008) *J. Clin. Invest.* **118,** 2347–2364
33. Gusarova, V., Seo, J., Sullivan, M. L., Watkins, S. C., Brodsky, J. L., and Fisher, E. A. (2007) *J. Biol. Chem.* **282,** 19453–19462
34. Shelness, G. S., and Ledford, A. S. (2005) *Curr. Opin. Lipidol.* **16,** 325–332
35. Gassama-Diagne, A., Yu, W., ter Beest, M., Martin-Belmonte, F., Kierbel, A., Engel, J., and Mostov, K. (2006) *Nat. Cell Biol.* **8,** 963–970
36. Krauss, M., and Haucke, V. (2007) *EMBO Rep.* **8,** 241–246
37. Orsó, E., Broccardo, C., Kaminski, W. E., Böttcher, A., Liebisch, G., Drobnik, W., Götz, A., Chambenoit, O., Diederich, W., Langmann, T., Spruss, T., Luciani, M. F., Rothe, G., Lackner, K. J., Chimini, G., and Schmitz, G. (2000) *Nat. Genet.* **24,** 192–196
38. Robenek, H., and Schmitz, G. (1991) *Arterioscler. Thromb.* **11,** 1007–1020
39. Schmitz, G., Assmann, G., Robenek, H., and Brennhausen, B. (1985) *Proc. Natl. Acad. Sci. U.S.A.* **82,** 6305–6309
40. Zha, X., Gauthier, A., Genest, J., and McPherson, R. (2003) *J. Biol. Chem.* **278,** 10002–10005
41. Kypreos, K. E. (2008) *Biochemistry* **47,** 10491–10502
42. Schaefer, E. J., Brousseau, M. E., Diffenderfer, M. R., Cohn, J. S., Welty, F. K., O'Connor, J., Jr., Dolnikowski, G. G., Wang, J., Hegele, R. A., and Jones, P. J. (2001) *Atherosclerosis* **159,** 231–236
43. Zha, X., Genest, J., Jr., and McPherson, R. (2001) *J. Biol. Chem.* **276,** 39476–39483
44. Joyce, C. W., Wagner, E. M., Basso, F., Amar, M. J., Freeman, L. A., Shamburek, R. D., Knapper, C. L., Syed, J., Wu, J., Vaisman, B. L., Fruchart-Najib, J., Billings, E. M., Paigen, B., Remaley, A. T., Santamarina-Fojo, S., and Brewer, H. B., Jr. (2006) *J. Biol. Chem.* **281,** 33053–33065
45. Brunham, L. R., Singaraja, R. R., Duong, M., Timmins, J. M., Fievet, C., Bissada, N., Kang, M. H., Samra, A., Fruchart, J. C., McManus, B., Staels, B., Parks, J. S., and Hayden, M. R. (2009) *Arterioscler. Thromb. Vasc. Biol.* **29,** 548–554